# MECHANICAL TEXTURISATION AND HYDROGEN PASSIVATION OF RGS (RIBBON GROWTH ON SUBSTRATE) SILICON SOLAR CELLS

G. Hahn, C. Zechner, M. Spiegel, W. Jooss, P. Fath, G. Willeke, E. Bucher
*Universität Konstanz, Fakultät für Physik, P.O.Box X916, D-78457 Konstanz, Germany*
*Tel.: +49-7531-88-3644, Fax: +49-7531-88-3895*
*E-mail: giso.hahn@uni-konstanz.de*

ABSTRACT**:** This study was carried out to enhance the performance of solar cells made from RGS Si, one of the most promising materials to deal with the Si feedstock problem.
Computer simulations predict a strong increase in $J_{sc}$ for materials with lower charge carrier diffusion lengths for solar cells including a mechanical texturisation step because of a higher charge carrier collection probability which has been shown for RGS solar cells.
Crystal defects present in RGS can be well passivated by a MIRHP (Microwave Induced Remote Hydrogen Plasma) passivation. In the present optimisation study on defect rich RGS material improvements in $V_{oc}$ of 80 mV, in $J_{sc}$ of 5.2 mA/cm$^2$ and in FF of 6% (FF=76%) led to an increase in $\eta$ of 2.7% absolute after MIRHP passivation.
For RGS material of standard quality a mechanical V-texturisation and MIRHP passivation step improves $V_{oc}$ (+12 mV), $J_{sc}$ (+2.4 mA/cm$^2$) and FF (+3.2% absolute) (including antireflection coating) as compared to an untextured reference cell without MIRHP passivation. The best RGS solar cell reported so far shows a $V_{oc}$ of 538 mV, $J_{sc}$ of 28.5 mA/cm$^2$, FF of 72.2% and an efficiency of $\eta$=11.1%. Further improvements are expected from solar cell optimisation as well as material improvements.
Keywords: Ribbons - 1: Passivation - 2: Texturisation - 3

## INTRODUCTION

Mechanical texturisation and a MIRHP (Microwave Induced Remote Hydrogen Plasma) passivation step are both well-known tools to enhance the performance of multicrystalline (mc) Si solar cells [1,2]. Especially cost effective ribbon Si materials containing more crystal defects than standard cast mc Si with lower minority charge carrier diffusion lengths $L_{diff}$ benefit from this treatment and cell parameters can be improved drastically [3]. In this study we have chosen RGS mc Si (supplied from Bayer AG) because of its capability to eventually reduce the Si feedstock shortage in photovoltaics. Its great advantage is the very fast production process without any material losses related to conventional wafer preparation [4].

## 1. MECHANICAL TEXTURISATION

The benefit of a textured surface for solar cells is twofold. The first advantage is the reduced reflectivity and better light trapping of long wavelength photons as compared to a flat surface. The second advantage is the enhanced charge carrier collection probability [1]. In order to investigate this effect quantitatively we carried out computer simulations for the charge carrier generation of the applied surface geometry [5]. Most charge carriers are created in the V-tip volume due to the inclined penetration of the light. Therefore the drift distance between the location of optical generation and the space charge region, the place of electrical generation is reduced. This causes an additional increase in $J_{sc}$ because more charge carriers can be collected before recombination. In Fig. 1 the results of two dimensional computer simulations for $J_{sc}$ and $V_{oc}$ in dependence of $L_{diff}$ are shown for a flat and a V-textured solar cell [6]. We assumed a single ARC (AntiReflection Coating) in both cases. While $J_{sc}$ is increased due to a higher collection probability, $V_{oc}$ slightly decreases especially for lower values of $L_{diff}$ due to the increased

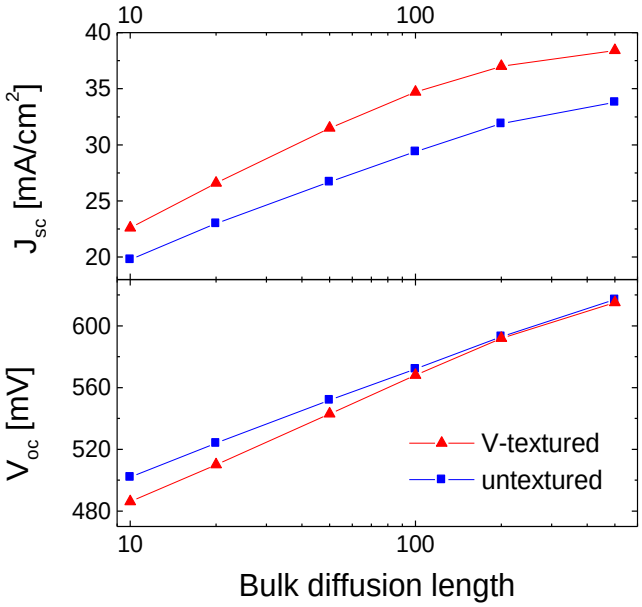


**Figure 1**: Two dimensional computer simulations showing the behaviour of $J_{sc}$ and $V_{oc}$ in dependence on the minority charge carrier bulk diffusion length of a flat and a V-grooved solar cell [6].

emitter area. This negative effect is negligible for larger diffusion lengths because the drop in $V_{oc}$ due to the larger emitter area can be fully compensated by the increase caused by the enhanced $J_{sc}$. For all values of $L_{diff}$ the simulations show an increase in efficiency for the V-textured cells.

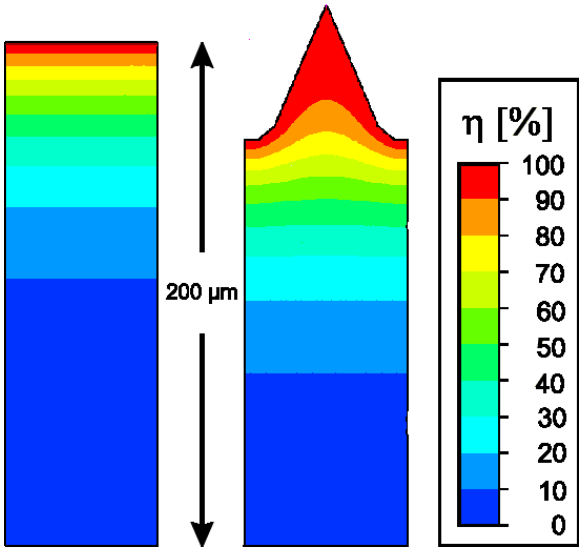


**Figure 2**: Charge carrier collection probability η of a 200 µm thick flat and a V-textured solar cell with an assumed $L_{diff}$ of 40 µm.

The best RGS solar cells in our study have a $L_{diff}$ of up to 40 µm after processing. In Fig. 2 the probability of a charge carrier being collected is shown in two dimensional profiles for a flat and a V-grooved cell structure. Especially in the V-tip volume the collection probability is strongly increased compared to the flat cell as can be seen by comparing the grey shadowed areas near the surface.

In Fig. 3 the V-grooved surface morphology of a processed RGS solar cell can be seen with a metal front grid finger running on a flat plateau.

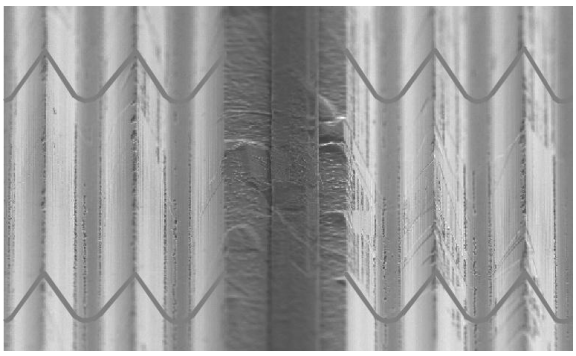

**Figure 3**: SEM picture of the surface of a V-grooved RGS solar cell with a grid finger running on top of a plateau.

## 2. MIRHP PASSIVATION

Defects in crystalline Si (grain boundaries, dislocations, etc.) can be passivated by indiffusion of atomic hydrogen. Especially mc ribbon Si materials show an increase in all cell parameters after a MIRHP passivation step [3]. In order to find out the optimum passivation time and temperature we carried out a passivation study on defect rich RGS material containing a high concentration of interstitial oxygen ($>3\cdot10^{18}$ $cm^{-3}$). The applied solar cell process is shown schematically in Fig. 4.

Planarisation
Defect etching
$POCl_3$ emitter diffusion
Thermal oxidation
Al gettering
Ti/Pd/Ag front contact (photolithographically defined)
Al back contact
MIRHP passivation

**Figure 4**: RGS solar cell process for the MIRHP passivation study on defect rich material.

The MIRHP passivation step was carried out after the metallization to be able to measure the benefit of this treatment on completed solar cells. Fig. 5 gives the increase in the solar cell parameters for four solar cells (2 x 2 $cm^2$) without ARC originating from the same RGS wafer.

Independent on the applied passivation temperature an increase in $V_{oc}$ of up to 80 mV could be observed. Higher temperatures lead to a faster passivation of the defects due to the higher diffusivity of hydrogen, but the same increase could be obtained for lower temperatures and longer passivation times. The influence of the passivation temperature and time on $J_{sc}$ is nearly identical to the one for $V_{oc}$, longer passivation times at lower temperatures lead to the same increase as short passivation times at higher temperatures. The behaviour of the fill factor (FF) is different. After an increase for all temperatures, FF is dropping significantly in dependence on the passivation temperature with higher temperatures causing a faster decrease. The largest improvements resulting in the highest FF (76%) for this process could only be obtained by longer passivation times at lower temperatures. Therefore the largest increase in efficiency was obtained by long passivation times at low temperatures (375° C). Higher temperatures lead to an indiffusion of metals from the front contact into the Si causing the observed drop in FF and $V_{oc}$. Nevertheless passivation at higher temperatures for shorter times could be used in a final RGS solar cell process when the optimum MIRHP passivation step is done before cell metallization.

The optimum passivation time and temperature seems to be a function of the concentration of interstitial oxygen present in the Si. Mc Si materials containing a lower amount of interstitial oxygen (eg. Edge-defined Film-fed Growth) can be completely passivated at considerably lower temperatures and passivation times as shown in another study [3][7]. Oxygen in interstitial form seems to play the role of an inhibitor for the atomic hydrogen during its diffusion into the Si bulk as demonstrated in [8].

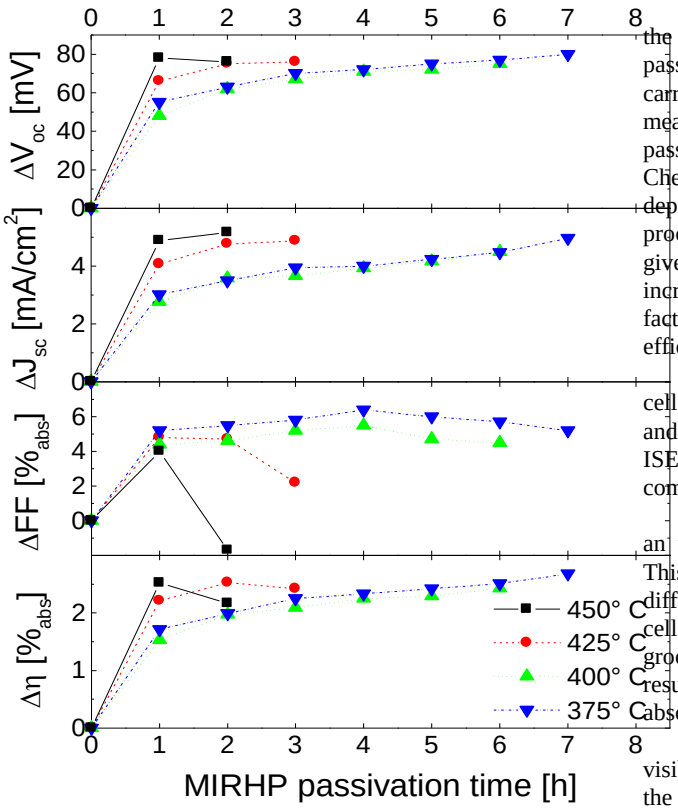


**Figure 5**: Improvement of RGS solar cell parameters after a MIRHP passivation step at different temperatures.

### 3. SOLAR CELL RESULTS

RGS wafers show sometimes differing properties concerning the diffusion length and the concentration of foreign atoms. In order to optimise the RGS solar cell process it is therefore necessary to compare cells from the same RGS wafer which shows itself an excellent homogeneity. In Table I cell parameters of four neighbouring solar cells originating from the same RGS wafer are shown. All cells are V-grooved without an ARC and a MIRHP step and only very small variations are visible.

**Table I**: IV-data of four V-grooved 2 x 2 $cm^2$ solar cells without ARC and MIRHP passivation step originating from the same RGS wafer with excellent homogeneity.

| | Cell 4a | Cell 4b | Cell 4c | Cell 4d |
|---|---|---|---|---|
| **$V_{oc}$ [mV]** | 513 | 508 | 511 | 511 |
| **$J_{sc}$ [mA/cm²]** | 22.9 | 22.5 | 22.7 | 22.9 |
| **FF [%]** | 72.2 | 72.3 | 72.2 | 72.2 |
| **η [%]** | 8.5 | 8.3 | 8.3 | 8.4 |

Crystal defects in RGS [9][10] can be very well passivated by a MIRHP passivation step [11] as shown in an earlier investigation [3]. Improvements of the best RGS Si material of up to 40 mV could be observed combined with a strongly increased $L_{diff}$ causing an increase of $J_{sc}$.

In order to prove this behaviour cells originating from the same RGS wafer with and without a MIRHP passivation step were compared. The passivation was carried out after cell metallization in order to be able to measure the cell parameters before and after the MIRHP passivation step. Afterwards a PECVD (Plasma Enhanced Chemical Vapour Deposition) $SiN_x/SiO_2$-DARC was deposited. A more detailed desciption of the RGS solar cell process is given in [12]. IV-results from this study are given in Table II. The MIRHP passivation step causes an increase in $V_{oc}$ of 27 mV, in $J_{sc}$ of 2.8 mA/$cm^2$ and in fill factor of 2.4% absolute resulting in an increase in efficiency of 1.9% absolute.

After the DARC deposition the V-grooved RGS solar cell including a MIRHP treatment shows a $V_{oc}$ of 538 mV and a record efficiency of 11.1% (certified at Fraunhofer ISE, Freiburg). This means an increase of 1.1% absolute compared to the cell without MIRHP step.

In Table II we also compare the V-textured cells with an untextured cell originating from another RGS wafer. This wafer showed similar properties concerning the diffusion length. Comparing the flat and the V-textured cells including double layer (D) ARC the mechanical V-grooving in combination with a MIRHP passivation step results in an overall increase in cell efficiency of 1.6% absolute.

The increase in $L_{diff}$ after the MIRHP treatment is also visible in spectral response data shown in Fig. 6 outlining the Internal Quantum Efficiencies (IQE) of the V-grooved cells before as well as after MIRHP step and DARC.

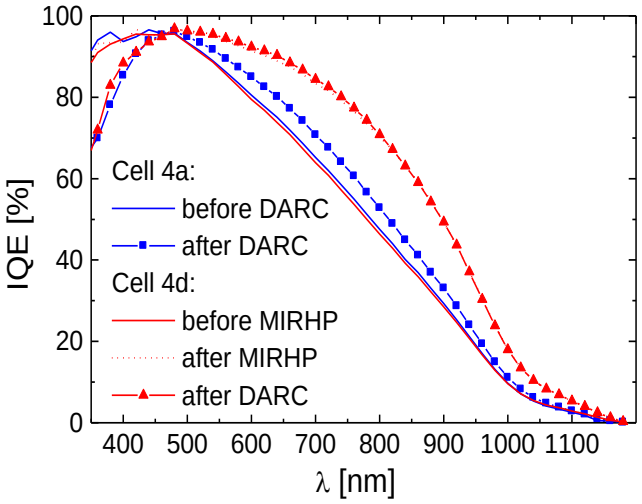


**Figure 6**: Spectral response data of two V-grooved RGS solar cells with and without a MIRHP passivation step before and after DARC.

Both cells (4a and 4d) originating from the same RGS wafer show nearly identical IQEs again proving the homogeneity of the wafer. After the MIRHP passivation step at 350° C for two hours (dotted line) the large increase of IQE in the long wavelength region is clearly visible. Fits in this region according to the method proposed by Basore [13] give an increase in $L_{diff}$ from 20 µm to approximately 40 µm. The subsequent deposition of a hydrogen rich $SiN_x/SiO_2$ DARC did not affect the long wavelength part of

the IQE but led to a drop of the IQE below 450 nm due to absorption and/or surface damaging.

**Table II**: IV-data of a flat and two V-grooved RGS solar cells with and without MIRHP passivation step.

| | Untextured cell 9c | | V-grooved cell 4a | | V-grooved cell 4d | | |
|---|---|---|---|---|---|---|---|
| | no DARC | DARC | no DARC | DARC | no DARC | MIRHP | MIRHP, DARC |
| **$V_{oc}$ [mV]** | 511 | 526 | 513 | 517 | 511 | 538 | 538 |
| **$J_{sc}$ [mA/cm$^2$]** | 17.4 | 26.1 | 22.9 | 27.1 | 22.9 | 25.7 | 28.5 |
| **FF [%]** | 71.1 | 69.2 | 72.2 | 71.2 | 72.2 | 74.6 | 72.4 |
| **$\eta$ [%]** | 6.3 | 9.5 | 8.5 | 10.0 | 8.4 | 10.3 | 11.1 |

The deposition of the same DARC for cell 4a (without the MIRHP passivation step) led to the same drop in the short wavelength part of the IQE but to a slight increase in the long wavelength part. This is due to the passivating properties of the hydrogen rich $SiN_x$ [14]. This additional increase can not be found for cell 4d besause the defects are already passivated after the MIRHP treatment.

## CONCLUSION

We implemented a V-groove texturisation and a MIRHP passivation step in our RGS solar cell process. The V-texture led to a higher $J_{sc}$ due to less reflection and a higher charge carrier collection probability as predicted by computer simulations when comparing textured cells with a flat reference cell originating from a RGS wafer with similar properties.

The benefits of RGS solar cell parameters in dependence on the MIRHP passivation temperature and time were investigated on defect rich RGS material. Lower passivation temperatures (375° C) led to the strongest increases in FF of up to 76% combined with the highest gain in efficiency.

A MIRHP passivation step after metallization for the best RGS quality material resulted in a largely increased $L_{diff}$ which could be demonstrated by spectral response measurements. An increase in $J_{sc}$, $V_{oc}$ and fill factor led to an increase in $\eta$ of 1.9% absolute.

Combining the V-grooving and the MIRHP passivation an efficiency for RGS of 11.1% could be reached which is the highest value so far reported for that Si material.

## ACKNOWLEDGEMENTS

We like to thank M. Steiner for SEM pictures and M. Keil for technical assistance during solar cell processing. The complementary supply of RGS ribbons from Bayer AG and the fruitful discussion with H.-U. Höfs and C. Häßler is gratefully acknowledged. This work was supported within the JOULE program of the European Commission under contract number JOR3-CT 95-0030.

## REFERENCES

[1] S. R. Wenham, PhD Thesis, University of New South Wales, 1986

[2] L. A. Verhoef, P.-P. Michiels, W. C. Sinke, C. M. M. Denisse, M. Hendriks, R. J. C. van Zollingen, Appl. Phys. Lett. **57** (25), 1990, 2704

[3] G. Hahn, W. Jooss, M. Spiegel, P. Fath, G. Willeke, E. Bucher, Proc. 26th IEEE PSC, Anaheim 1997, 75

[4] H. Lange, I. A. Schwirtlich, J. Cryst. Growth **104** (1990) 108

[5] C. Gerhards, C. Marckmann, R. Tölle, P. Fath, G. Willeke, E. Bucher, Proc. 26th IEEE PSC, Anaheim 1997, 43

[6] C. Zechner, P. Fath, G. Willeke, E. Bucher, Proc. 14th EC PVSEC, Barcelona 1997, 69

[7] M. Spiegel, G. Hahn, W. Jooss, S. Keller, P. Fath, G. Willeke, E. Bucher**,** this conference

[8] H. E. A. Elgamel, J. Poortmans, J. Nijs, R. Mertens, P. Fath, M. Goetz, Proc. 9th PVSEC, Miyazaki 1996, 103

[9] H. J. Möller, M. Gosh, M. Rinio, S. Riedel, D. Yang, Proc. 13th EC PVSEC, Nizza 1995, 1390

[10] G. Hahn, M. Spiegel, S. Keller, A. Boueke, P. Fath, G. Willeke, E. Bucher, Proc. 14th EC PVSEC, Barcelona 1997, 81

[11] M. Spiegel, P. Fath, K. Peter, B. Buck, G. Willeke, E. Bucher, Proc. 13th EC PVSEC, Nizza 1995, 421

[12] G. Hahn, C. Zechner, B. Bitnar, M. Spiegel, W. Jooss, P. Fath, G. Willeke, E. Bucher, H.-U. Höfs, Prog. Photovolt., **6** (3), 1998, 163

[13] P. A. Basore, Proc. 23rd IEEE PSC, Louisville, 1993, 147

[14] L. Cai, A. Rohatgi, IEEE Trans. Electr. Dev., **44** (1), 1997, 97